Journal of the Optical Society of America B
OPTICAL PHYSICS

Wigner's phase space current for variable beam splitters—seeing beam splitters in a new light

OLE STEUERNAGEL[1,*] AND RAY-KUANG LEE[1,2,3,4,5]

[1]Institute of Photonics Technologies, National Tsing Hua University, Hsinchu 30013, Taiwan
[2]Department of Physics, National Tsing Hua University, Hsinchu 30013, Taiwan
[3]Center for Theory and Computation, National Tsing Hua University, Hsinchu 30013, Taiwan
[4]Center for Quantum Science Technology, Hsinchu 30013, Taiwan
[5]rklee@ee.nthu.edu.tw
*Ole.Steuernagel@gmail.com

Received 22 October 2024; revised 25 November 2024; accepted 25 November 2024; posted 26 November 2024; published 3 January 2025

Beam splitters allow us to superpose two continuous single-mode quantum systems. To study the behavior of their strong mode mixing dynamics, we consider variable beam splitters and their dynamics using Wigner's phase space distribution, W, the evolution of which is governed by the continuity equation $\frac{\partial}{\partial\tau}W=-\nabla\cdot\boldsymbol{J}$. We derive the form of the corresponding Wigner current, $\boldsymbol{J}$, of each outgoing mode after tracing out the other. The influence of the modes on each other is analyzed and visualized using their respective Wigner distributions and Wigner currents. This allows us to perform geometrical analyses of the mode interactions, casting new light on beam splitter behavior. Several of the presented results should be immediately testable in experiments.

https://doi.org/10.1364/JOSAB.545875

1. INTRODUCTION

In quantum optics, beam splitters are often used to entangle two matched modes [1] in order to study the behavior of one outgoing mode conditioned on the state of the other. Such studies traditionally focus on the states alone, typically in Fock space or using phase space representations [2–4].

Here, we show that, instead of focusing on the state alone, it can be useful to complement such studies by describing and visualizing the dynamics of the beam splitter interaction using Wigner's phase space current, $\boldsymbol{J}$ [5–9], thus presenting beam splitter behavior in a new light.

Wigner's description of quantum systems [10] in phase space, based on Wigner's distribution $W(x,p)$, has given us visualizations comparing classical with quantum states [11–16]. Moreover, the associated Wigner current, $\boldsymbol{J}$, can be constructed from a variable beam splitter's fictitious time evolution [9,17] and allows for a direct visualization of the system dynamics and its comparison with classical Hamiltonian flows [6,18,19]. No such current exists to describe ρ's evolution (no one studies the commutator $[\hat{H},\hat{\rho}]$ by itself).

Since the state space for two optical modes is four-dimensional, we trace out either mode and study the behavior of the remaining mode through its two-dimensional Wigner distribution and current. This allows us to study and visualize the behavior of such systems using the phase space current vector fields, $\boldsymbol{J}$, and their "quantum phase portraits" (as two-dimensional plots). By tracing out one mode, we derive the expressions for the "effective Moyal brackets" [16,20–22] and the form of Wigner's phase space current for the other mode.

We highlight two aspects whose investigation should become experimentally accessible [9]: the inversion of the direction of the Wigner current [6,7] associated with the presence of areas in phase space where the Wigner distribution is negative, and the pronounced violation of phase space volume conservation [23] in quantum dynamics.

We emphasize that superposing perfectly matched [1] modes at a mixing beam splitter is governed by one of the simplest coupling dynamics one can think of. By themselves, matched modes evolve as equal harmonic oscillators, and their dynamics can be factored out, while their two-mode interaction Hamiltonian is simple and bilinear in the modes; see Eq. (8). This permits us to study how superposed beam splitter modes influence each other without the complicating effects of a complicated system's intrinsic dynamics [7,19,24], allowing us to pinpoint the details of the mechanism by which mode entanglement is responsible for the non-classical behavior [25,26] observed in beam splitter interactions.

Classical mechanics has benefited enormously from the study of classical phase space portraits [27]. In the quantum case, phase space-based approaches allow for the study of "quantum phase portraits" (collections of momentary snapshots of field lines arising from the integration of the vector field $\boldsymbol{J}$ [6,18]). There is no other formulation of quantum theory [28] that allows for such an intuitive way of studying quantum dynamics and is so reminiscent of classical dynamics studies [20]. Plotting

$\boldsymbol{J}$ and its quantum phase space portraits allows us to apply geometrical reasoning that sheds new light on the behavior of beam splitters.

Section 2 introduces Wigner's continuity equation and phase space current, $\boldsymbol{J}$. In Section 3, we derive its form for variable beam splitters. Section 4 presents several examples and highlights interesting features of their phase space dynamics. Subsection 4.B highlights the occurrence of singular phase space volume changes, and Subsection 4.C shows that this is due to mode entanglement. Our conclusions, in Section 5, put our findings into context.

2. WIGNER DISTRIBUTION AND ITS CONTINUITY EQUATION

At first glance, it might appear that the study of conditional dynamics, since it involves sudden "collapses" due to measurements, seems to leave no room for a continuous description by a continuity equation with a current $\boldsymbol{J}$. After all, we know that Schrödinger's equation does not describe measurement collapses.

And yet, in experiments, we often change a system parameter continuously such that, instead of physical time, we study the dependence on this parameter, playing the role of an "effective time" in a fictitious evolution [9,17]. And we execute the measurement, inducing a collapse, after the parameter-mediated interaction is over. In this case, we can still characterize the behavior of a system as continuously evolving (and then being terminated by a measurement [9]).

The time evolution of Wigner's quantum phase space distribution $W(x,\,p,\,\tau)$ [29,30], for a one-dimensional continuous system, is governed by its phase space current $\boldsymbol{J}$ and obeys the continuity equation [23,31,32]:

$$\frac{\partial W(x,\,p,\,\tau)}{\partial \tau} + \boldsymbol{\nabla}\cdot\boldsymbol{J}(x,\,p,\,\tau) = 0, \tag{1}$$

where $\boldsymbol{\nabla} = (\frac{\partial}{\partial_x},\,\frac{\partial}{\partial_p})$ is the phase space divergence operator with respect to position x and momentum p, τ is time, and $\boldsymbol{J} = (J_x,\,J_p)^{\intercal}$ has two components and is a function of W and the system Hamiltonian $H(x,\,p,\,\tau)$.

We specifically study the use of beam splitters as mode mixers. Small variations in reflectivity r allow us to invoke a continuous description using an effective Hamiltonian and thus the continuity equation (1) [33].

In our approach, the study of details and changes of the Wigner distributions is underpinned by plots of their phase space current $\boldsymbol{J}$ together with $\boldsymbol{J}$'s field lines. This complements the standard treatment of beam splitter behavior in terms of photon statistics [2] or their effects on wavefunctions [3].

3. CURRENT $\boldsymbol{J}$ FROM MOYAL'S BRACKET

We will now remind the reader of how Wigner's and Schrödinger's formulations of quantum theory are connected mathematically [16].

Consider a single-mode operator given in coordinate representation $\langle x-y|\hat{O}|x+y\rangle = O(x-y,\,x+y)$. To map to Wigner's phase space formulation, we employ the Wigner transform, $\mathcal{W}[\hat{O}]$, [16,20,34]:

$$\mathcal{W}[\hat{O}](x,\,p) = \int_{-\infty}^{\infty} \mathrm{d}y\; O\left(x-\frac{y}{2},\,x+\frac{y}{2}\right)\,\mathrm{e}^{\frac{\mathrm{i}}{\hbar}py}. \tag{2}$$

If $\hat{O}$ is a (normalized) single-mode density matrix $\hat{\rho}$, then the associated normalized distribution in the Wigner formulation is the Wigner distribution:

$$W(x,\,p,\,\tau) \equiv \frac{\mathcal{W}[\hat{\rho}]}{2\pi\hbar}. \tag{3}$$

The Wigner transform of the von Neumann time evolution equation $\mathcal{W}[\frac{\partial\hat{\rho}}{\partial\tau} = \frac{1}{\mathrm{i}\hbar}[\hat{H},\,\hat{\rho}]]$ is

$$\frac{\partial W}{\partial \tau} = \{\{H,\,W\}\}, \tag{4}$$

in which the Groenewold–Moyal bracket [16,21,22] is the quantum version of the Poisson bracket with the explicit form:

$$\{\{f,\,g\}\} = \frac{2}{\hbar} f(x,\,p)\,\sin\left[\frac{\hbar}{2}\left(\frac{\overleftarrow{\partial}}{\partial x}\frac{\overrightarrow{\partial}}{\partial p} - \frac{\overleftarrow{\partial}}{\partial p}\frac{\overrightarrow{\partial}}{\partial x}\right)\right] g(x,\,p), \tag{5}$$

where arrows indicate the "direction" of differentiation: $f\frac{\overrightarrow{\partial}}{\partial x}g = g\frac{\overleftarrow{\partial}}{\partial x}f = f\frac{\partial}{\partial x}g$.

Equation (4) can be rewritten as the divergence of Wigner's phase space current [7,23,35], yielding Eq. (1).

A. Contrast with Schrödinger Equation

We note that Eq. (1) is the Fourier transform [Eq. (2)] of the von Neumann equation (4), just as $W(x,\,p)$ is the Fourier transform of the density matrix $\rho(x,\,x')$.

The Fourier transform [Eq. (2)] is invertible; in fact, it is a unitary map: Wigner's and the Schrödinger–von Neumann formulation are therefore *unitarily equivalent*.

Additionally, to the Schrödinger–von Neumann formulation, Wigner's formulation of quantum theory has the great advantage of allowing us to visualize quantum dynamics in phase space more directly since W is real-valued [30,36,37]. Compared to other quantum phase space distributions [38], Wigner's [10] is special [39–41] and intuitive [37,42]; here, we use it exclusively.

Additionally, unlike formulations of quantum physics that are not based on phase space [28], Wigner's formulation allows us to use the continuity equation (1), and hence Wigner's phase space current $\boldsymbol{J}$ and its quantum phase portraits.

Recent experimental work shows that the reconstruction of Wigner's phase space current $\boldsymbol{J}$ and its effects on the evolution of the system can be studied with high resolution [9].

B. Beam Splitter and Its Effective Hamiltonian

We consider an ensemble of measurements performed on a system of two modes $\hat{a}$ and $\hat{b}$, which arise from perfectly matched incoming modes a_{in} and b_{in} after being mixed through interaction at a "perfect" lossless two-mode beam splitter with variable transmissivity.

The associated unitary mode mixing operator [2,43], transforming the bosonic optical-mode field operators,

$$\begin{pmatrix}\hat{a}\\ \hat{b}\end{pmatrix} = \hat{B}(\theta)\begin{pmatrix}\hat{a}_{\rm in}\\ \hat{b}_{\rm in}\end{pmatrix}\hat{B}^\dagger(\theta), \tag{6}$$

is given by

$$\hat{B}(\theta) = \exp\left[\frac{\theta}{2}\left(\hat{a}_{\rm in}\hat{b}^\dagger_{\rm in} - \hat{a}^\dagger_{\rm in}\hat{b}_{\rm in}\right)\right] \equiv \exp\left[-{\rm i}\tau\,\hat{H}_M\right], \tag{7}$$

with the effective Hamiltonian

$$\hat{H}_M = {\rm i}\frac{\pi}{2}\left(\hat{a}_{\rm in}\hat{b}^\dagger_{\rm in} - \hat{a}^\dagger_{\rm in}\hat{b}_{\rm in}\right) = \frac{\pi}{2}\left(\hat{x}_a\hat{p}_b - \hat{p}_a\hat{x}_b\right). \tag{8}$$

Our choices (together with the fact that the reflection amplitude is $r = \sin(\frac{\pi}{2}\tau)$, and $t = \cos(\frac{\pi}{2}\tau)$ is the transmission amplitude) allow us to choose the range $\tau \in [0, 1]$, which parameterizes the behavior, ranging from no mode-mixing at $\tau = 0$ (complete transparency) via all intermediate values, where the modes are being mixed, to eventually no mixing at $\tau = 1$, due to total reflection at the beam splitter.

In an implementation of the variable beam splitter as a two-mode fiber coupler, τ parameterizes the coupling length; implemented as a Mach–Zehnder interferometer it parameterizes changes of the phase shifter angle.

The Wigner transform of the associated von Neumann equation gives the evolution equation of the two-mode Wigner distribution $W_{ab} = W_{ab}(x_a, p_a, x_b, p_b, \tau)$:

$$\frac{\partial\mathcal{W}[\hat{\rho}]}{\partial\tau} = 2\pi\hbar\frac{\partial W_{ab}}{\partial\tau} = \mathcal{W}\left[\frac{\pi}{2{\rm i}\hbar}\left[\left(\hat{x}_a\hat{p}_b - \hat{p}_a\hat{x}_b\right), \hat{\rho}_{ab}\right]\right]. \tag{9}$$

C. Wigner Current for Mixed Modes

Let us assume that we choose mode a as auxiliary, to be traced out of the state $\hat{\rho}_{ab}$. Then the Wigner transform of the von Neumann equation (9) for the partial trace density matrix $\hat{\rho}_b$, occupying the remaining mode b, is

$$2\pi\hbar\frac{\partial W_b}{\partial\tau} = \frac{\pi}{2}\mathcal{W}\left[\frac{1}{{\rm i}\hbar}{\rm Tr}_a\{[\hat{x}_a\hat{p}_b, \hat{\rho}_{ab}] - [\hat{p}_a\hat{x}_b, \hat{\rho}_{ab}]\}\right], \tag{10}$$

and hence, using the cyclicity of the trace and Eqs. (3) and (4),

$$\frac{\partial W_b}{\partial\tau} = \frac{\pi}{2}\left(\{\{p_b, {\rm Tr}_a\{x_a W_{ab}\}\}\} - \{\{x_b, {\rm Tr}_a\{p_a W_{ab}\}\}\}\right), \tag{11}$$

where $\{\{p_b, {\rm Tr}_a\{x_a\bullet\}\}\}$ and $\{\{-x_b, {\rm Tr}_a\{p_a\bullet\}\}\}$ are the "effective Moyal brackets" taking W_{ab} as an argument; see Eq. (4).

Applying Eq. (5) leads to

$$\frac{\partial W_b}{\partial\tau} = -\frac{\pi}{2}\left[x_b\frac{\overleftarrow{\partial}}{\partial x_b}\frac{\overrightarrow{\partial}}{\partial p_b}{\rm Tr}_a\{p_a W_{ab}\} + p_b\frac{\overleftarrow{\partial}}{\partial p_b}\frac{\overrightarrow{\partial}}{\partial x_b}{\rm Tr}_a\{x_a W_{ab}\}\right]. \tag{12}$$

According to the continuity equation (1), this is rewritten as [7,23,35]

$$\frac{\partial W_b}{\partial\tau} = -\frac{\pi}{2}\begin{pmatrix}\frac{\partial}{\partial x_b}\\ \frac{\partial}{\partial p_b}\end{pmatrix}\cdot\begin{pmatrix}{\rm Tr}_a\{x_a W_{ab}\}\\ {\rm Tr}_a\{p_a W_{ab}\}\end{pmatrix} = -\nabla_b\cdot\boldsymbol{J}_b, \tag{13}$$

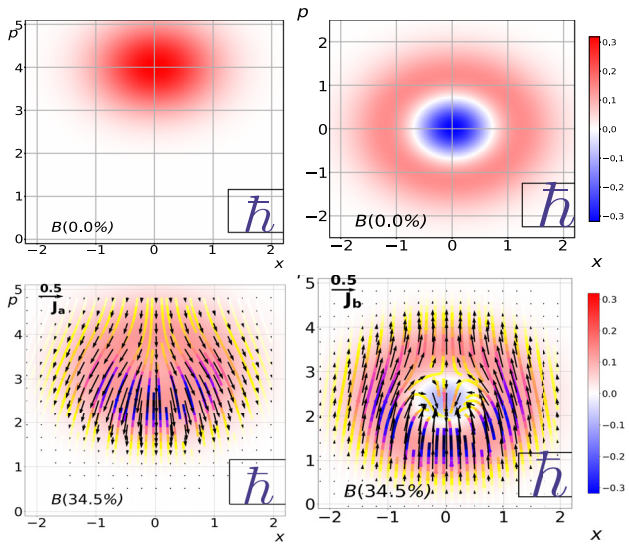

Fig. 1. Wigner distributions $W_{a\backslash b}$ of modes a (left panels) and b (right panels). The top row shows the initial states, and the bottom row shows the evolved states together with their vector fields $\boldsymbol{J}_{a\backslash b}$ as overlays. As a guide to the eye, the $\boldsymbol{J}$-fields are integrated, yielding white-yellow-blue (coloring according to $|\boldsymbol{J}|$) field lines that represent momentary snapshots of the $\boldsymbol{J}$-fields. Thick black frames surround an area of size $\boxed{\hbar}$ in phase space. $B(34.5\%)$ represents mixing at a beam splitter with 34.5% reflectivity. The initial states are a coherent state and a single-photon Fock state: $|\psi_a\rangle|\psi_b\rangle = |\alpha = 4{\rm i}/\sqrt{2}\rangle \otimes |1\rangle$.

where the Wigner current of mode b, conditioned on the state of mode a, is

$$\boldsymbol{J}_b(x_b, p_b, \tau) = +\frac{\pi}{2}\begin{pmatrix}{\rm Tr}_a\{x_a W_{ab}\}(x_b, p_b, \tau)\\ {\rm Tr}_a\{p_a W_{ab}\}(x_b, p_b, \tau)\end{pmatrix}. \tag{14}$$

An analogous calculation yields the Wigner current, $\boldsymbol{J}_a$, of mode a, conditioned on the state of mode b, as

$$\boldsymbol{J}_a(x_a, p_a, \tau) = -\frac{\pi}{2}\begin{pmatrix}{\rm Tr}_b\{x_b W_{ab}\}(x_a, p_a, \tau)\\ {\rm Tr}_b\{p_b W_{ab}\}(x_a, p_a, \tau)\end{pmatrix}. \tag{15}$$

D. Contrast with Classical Mechanics

We would like to stress that, despite the existence of continuity equations, currents, and phase portraits in quantum phase space formulations [5,6,18,31,32,44,45], in general, trajectories in quantum phase space do *not exist* [23]. We neither discuss paths (such as Feynman's, which do not have to follow equations of motion) nor center-of-mass trajectories, as famously discussed by Heisenberg in his 1927 paper on interpretations of *observed* particle trajectories [46].

We remind the reader that trajectories are integral curves that obey the equations of motion *and* describe the transport of probability. In quantum mechanics, these do not generally exist since phase space velocities would develop singularities [23].

Although trajectories do not exist, we can determine phase space field lines, the integral curves of $\boldsymbol{J}$ at a fixed time; see the lower panels of Fig. 1 (and also Fig. 3). Specifically, in classical mechanics' phase space settings, such curves are also known as phase curves, and their collection as phase portraits, which is

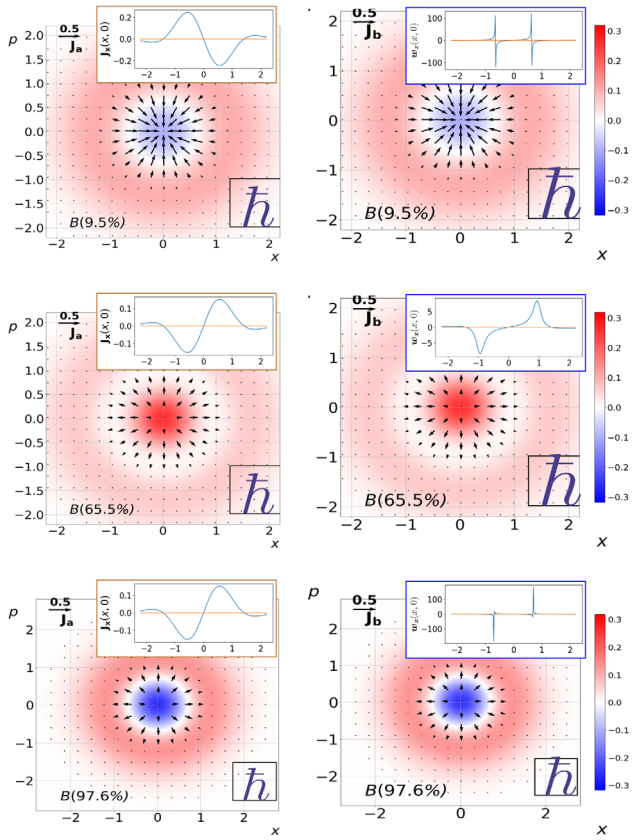

Fig. 2. Layout as in Fig. 1. The initial states are two single-photon Fock states: $|\psi_a\rangle|\psi_b\rangle = |1\rangle \otimes |1\rangle$ (see the top right panel of Fig. 1), and the modes a and b behave identically. Insets in the panels on the left column (brown frames) show plots of the x component $\boldsymbol{J}_x(x, 0)$ along the x axis. Insets in the panels on the right column (blue frames) show plots of the x component $\boldsymbol{w}_x(x, 0)$ along the x axis and that it is singular when $W = 0$.

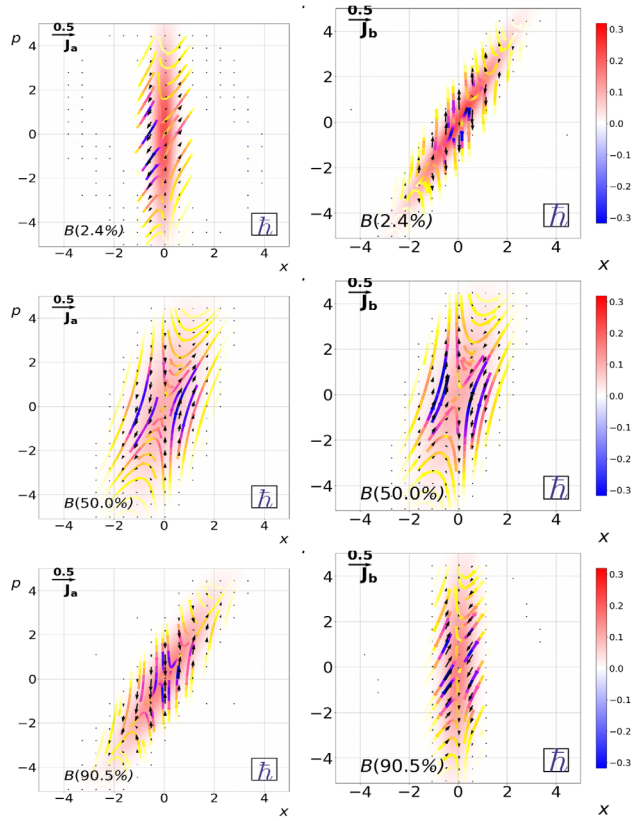

Fig. 3. Layout as in Fig. 1, with two equally strongly squeezed vacua: $|\psi_a\rangle|\psi_b\rangle = |z = 2, \theta = 0\rangle \otimes |z = 2, \theta = -\pi/3\rangle$ as initial states.

why we introduce the term "quantum phase portraits" to denote such collections of field lines.

Let us briefly explain why singular volume changes occur in quantum phase space. In classical physics, the current factorizes into density and the classical phase space velocity field [23] $\boldsymbol{j} = \rho \boldsymbol{v}$; therefore, $\boldsymbol{v} = \boldsymbol{j}/\rho$. In quantum dynamics, however, attempting this approach, namely, defining the quantum phase space velocity field, $\boldsymbol{w} = \boldsymbol{J}/W$, typically yields singular values somewhere in phase space since the Moyal bracket contains derivatives of W, which is why zeros of W do not need to coincide with those of $\boldsymbol{J}$; see Fig. 2. Therefore, the degeneracy between zeros of W and $\boldsymbol{J}$ is typically lifted, and when W is zero, $\boldsymbol{w} = \boldsymbol{J}/W$ is singular; see insets in the right column of Fig. 2. Liouville's classical phase space volume conservation is described by the condition $\nabla \cdot \boldsymbol{v} = 0$; the equivalent quantum expression $\nabla \cdot \boldsymbol{w}$ can assume values with infinite magnitude [23].

This causes trajectory approaches to be flawed, as they are based on $\boldsymbol{w}$, and so they develop singularities and singular changes in phase space volumes when $W = 0$; in short, there are no trajectories in quantum phase space [23].

One should avoid using the unfortunate term "quantum Liouville equation," which has caused great confusion when researchers talk about so-called "quantum characteristics" in phase space and try to implement trajectories-based code on computers [23]. Instead, correctly set up and efficient "exact" numerical codes for the propagation of Wigner's distribution using spectral methods do exist [47], also in the case of nonlinear wave equations [24] and nonseparable Hamiltonians [48].

4. RESULTS FOR VARIOUS FIELD STATES

In this section, we consider initially unentangled states $|\psi_a\rangle|\psi_b\rangle = |\psi_a\rangle \otimes |\psi_b\rangle$ for the incoming beam splitter modes $a_{\rm in}$ and $b_{\rm in}$, using the following notation:

N-photon Fock states are denoted by $|N\rangle$, degenerate squeezed vacuum states $\exp[\frac{1}{2}(\zeta^* \hat{a}^2 - \zeta \hat{a}^{\dagger 2})]|0\rangle$ by $|z = |\zeta|, \theta = \arg(\zeta)\rangle$, and Glauber coherent states $\exp[\alpha \hat{a}^\dagger - \alpha^* \hat{a}]|0\rangle$ by $|\sqrt{2}\alpha = x + \mathrm{i}p\rangle$.

A. Energy and Purity Changes

Figure 1 illustrates that the modes can exchange energy: mode a loses and b gains energy. The $\boldsymbol{J}$-fields are integrated, yielding white-yellow-blue field lines that expand and converge, hinting at the fact that phase space volumes are not conserved [23].

Let us consider roughly balanced beam splitters for mixing modes, with initial states such as two single photons or different squeezed states. It is known that for such strongly mixing beam splitters, the modes become strongly entangled with each other (Fig. 2 describes Hong–Ou–Mandel interference [49]), while the individual modes become fairly impure by themselves: throughout phase space, the distributions $W_{a\backslash b}$ become positive and widely spread out; see Figs. 2 and 3.

Here, the Wigner current patterns can reveal further details of such purity destroying dynamics [25]. In the top row of Fig. 2, the central inflow fills the negative region around the origin without affecting the positive torus very much, leading to fully mixed states (middle row).

B. Changes in Phase Space Volumes

It is known that the formation of "negative regions," where the Wigner distribution has negative values, implies that phase space volumes are not conserved. Here, this is underpinned in a visual way by the observation of radially outward- or inward-pointing star-current patterns; see Figs. 1 and 2. According to Gauss' law (or the flux theorem), this implies the existence of sources or sinks of the local probability current $\boldsymbol{J}$. Such local changes of Wigner's quasi-probability density distribution are alien to classical physics but required in the quantum case, also for conservative systems [23].

In the case of Fig. 2, we can explicitly consider this lack of volume conservation. The current fields are strictly radial, but the insets in the panels of the right column of Fig. 2 show that the magnitude of $\boldsymbol{w}$ does *not* drop off with the inverse radius $R^{-1} = 1/\sqrt{x^2 + p^2}$. Thus, $\nabla \cdot \boldsymbol{w} \neq 0$, and quantum phase space volumes are not conserved. This is not necessarily surprising since we look at a subsystem of a coupled system and tracing out the partner system means that the subsystem is not governed by a conservative Hamiltonian. However, what is impossible in classical physics is the occurrence of singular velocity fields [23]; see the explanation in Section 3.D and the insets in the right column of Fig. 2.

In the next subsection, we explain the occurrence of singular phase space volume changes and their connection with mode entanglement.

C. Negative Values of *W* from Entanglement

For beam splitters, the Liouville condition for phase space volume conservation can be *maximally violated*; phase space volume changes can be singular: $|\nabla \cdot \boldsymbol{w}| = \infty$. We explained the possibility for such singularities occurring in terms of the lifting of the degeneracy in the formation of zeros of $\boldsymbol{J}$ and W; see Subsection 3.D.

Yet, at a first careless glance, it is surprising to find singularities in $\boldsymbol{w}$ for Hamiltonians [Eq. (8)] *bilinear* in x and p since only the "classical" looking linear term [23,50] of the Moyal bracket [Eq. (5)] is present in evolution equation (12).

Why do we find singularities in $\boldsymbol{w}$ (such as those shown in the insets of the right column of Fig. 2)?

The reason is mode entanglement [25,26]:

The system can form zeros in W while, simultaneously, $\boldsymbol{J}$ does not vanish. Again, the degeneracy in the formation of zeros of $\boldsymbol{J}$ and W are lifted, causing singularities in $\boldsymbol{w}$. As a generic example, let us consider the x component of $\boldsymbol{J}_b$ [Eq. (14)]. It is proportional to $\mathrm{Tr}_a\{x_a W_{ab}\}(x_b, p_b, \tau)$, and this expression is generally *not proportional* to W_b, if modes a and b are *entangled*. Hence, when W_b forms a negative region, it vanishes on the boundary of that region, and there $\boldsymbol{w}_b = \boldsymbol{J}_b / W_b$ can form singularities.

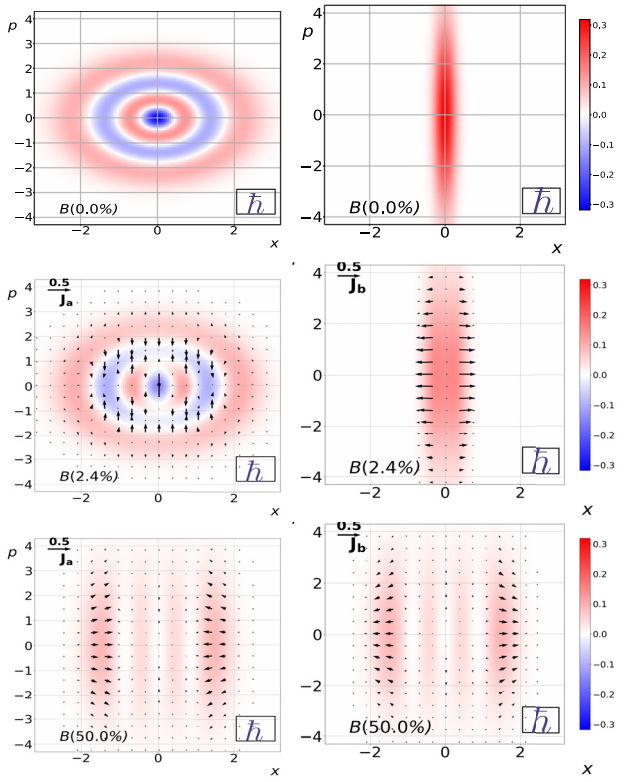

Fig. 4. Layout as in Fig. 1. The initial state is a three-photon Fock state and squeezed vacuum: $|\psi_a\rangle|\psi_b\rangle = |3\rangle \otimes |z = 1.2, \theta = 0\rangle$.

Such singular phase space volume changes, or rather, their signature—nonzero $\boldsymbol{J}$, while the density W vanishes—have so far not been observed experimentally.

D. Phases and Fluctuations

We remark that it might seem surprising to note that Eqs. (15) and (14) for $\boldsymbol{J}_a$ and $\boldsymbol{J}_b$ are of the same mathematical form if the indices a and b are swapped, except for the presence of a minus sign for $\boldsymbol{J}_a$. Yet, $\boldsymbol{J}_a$'s and $\boldsymbol{J}_b$'s current plots in Fig. 2 are identical. This is due to the fact that the definitions of the beam splitter modes carry relative phases that are imprinted within W_{ab}, correctly compensating for $\boldsymbol{J}_a$'s minus sign.

Figure 3 shows that the squeezed states affect each other in a geometrically transparent fashion: the large fluctuations in the direction of the anti-squeezed quadrature dominate the direction in which the current broadens the state in the other mode. This type of geometrical reasoning also explains qualitatively how the symmetry breaking seen in the left column of Fig. 4 arises: the non-classical phase space-interference fringes [14] in the a-mode's Fock state wash out more quickly in the p direction than the x direction since the b-mode is squeezed in its x direction and anti-squeezed in p.

We remark that, according to Eqs. (14) and (15), the beam splitter [Eq. (7)] only mixes the positions x_a and x_b with each other, and the momenta p_a and p_b with each other. There is no cross-mixing of positions with momenta [3].

It is not always obvious how Eqs. (14) and (15) for $\boldsymbol{J}_b$ and $\boldsymbol{J}_a$ give rise to the described phenomena. After all, the relative

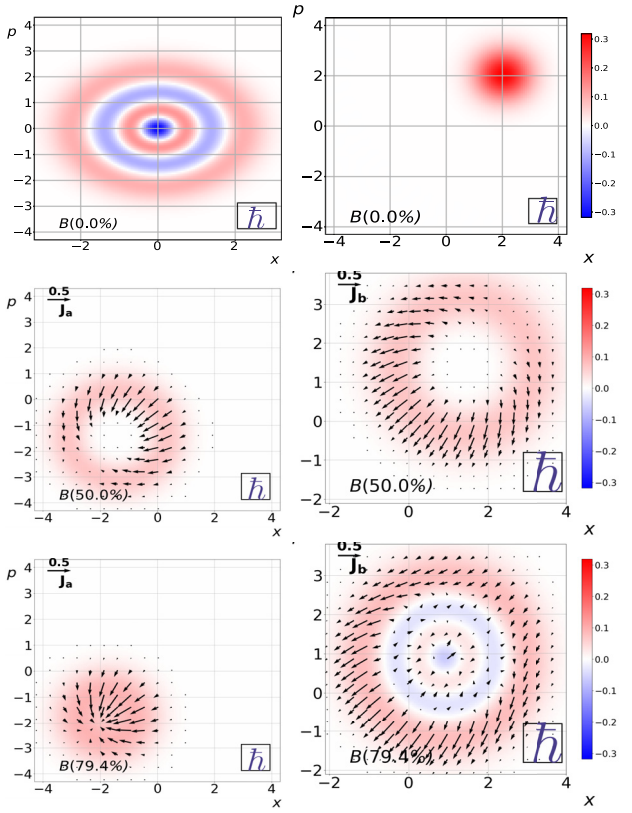

Fig. 5. Layout as in Fig. 1. The initial state is a three-photon Fock state and coherent state: $|\psi_a\rangle|\psi_b\rangle = |3\rangle \otimes |\alpha = 2(1+\mathrm{i})/\sqrt{2}\rangle$.

phases that govern the direction of the dynamics (another example, for a tunnelling scenario, can be found in the discussion around Fig. 2 of Ref. [6]) are "hidden" in the expressions for W_{ab} of Eqs. (14) and (15). In the case of Fig. 3, for example, initially (for small beam splitter reflectivities), the relative phases are such that the distributions become smeared out, but later on (for much greater reflectivities) the process, instead, narrows the distributions. All this, while the forms of Eqs. (14) and (15) remain unchanged, the expressions for W_{ab} have changed.

The Wigner current inverts its direction when W is negative [7], and such inversions (current moves against the prevailing direction) are clearly displayed in the lower right panels of Figs. 1 and 5.

5. CONCLUSION

We have shown how the Wigner current for coupled systems can be determined after tracing out one or the other subsystem. We specified this for the case of variable beam splitters and highlighted various aspects of the corresponding phase space dynamics. It is straightforward to apply the calculations in Section 3 to other forms of interaction Hamiltonians coupling two systems.

We emphasized that the effective Moyal brackets describing the conditional beam splitter dynamics show features familiar from systems coupled to environments far from thermal equilibrium: energy or purity are not conserved in each subsystem. Energy and purity can go up or down.

We specifically highlighted aspects of the quantum phase space dynamic, which our analysis has unearthed as being experimentally accessible when using variable beam splitters and which, in quantum optics, can be difficult to generate and experimentally investigate otherwise. These are: the formation of negative areas of the Wigner distributions, the inversion of Wigner's phase space currents associated with these negative areas, and the pronounced violation of phase space volume conservation [23] in quantum dynamics, which are all tied to the entanglement between the two mode [25,26].

Traditionally, states and how they change over time are studied; here we suggest to additionally use the vector fields $\boldsymbol{J}_a$ and $\boldsymbol{J}_b$. It allows us to apply *geometrical reasoning* to extract quantitative and qualitative information of how their interaction drives the system dynamics. This is one of the main findings of this work and one of its main motivations.

We hope that the approach laid out in this work can also lead to new ideas about how to tailor Hamiltonians [8] and states (here, depending on the "other mode" that is traced over) to generate interesting new quantum states and quantum dynamics. We anticipate that the geometrical reasoning demonstrated here can also be applied in other multimode cases with other couplings and will help with the detailed analysis of the dynamics of such systems, based on the analysis of Wigner's phase space current $\boldsymbol{J}$.

Funding. Ministry of Science and Technology of Taiwan (112-2123-M-007-001, 112-2119-M-008-007, 112-2119-M-007-006); Office of Naval Research Global; International Technology Center Indo-Pacific (ITC IPAC); Army Research Office (FA5209-21-P-0158); University of Tokyo.

Acknowledgment. This work was partially supported by the Ministry of Science and Technology of Taiwan, the Office of Naval Research Global, the International Technology Center Indo-Pacific (ITC IPAC) and Army Research Office, and the collaborative research program of the Institute for Cosmic Ray Research (ICRR) at the University of Tokyo.

Disclosures. The authors declare no conflicts of interest.

Data availability. Data underlying the results presented in this paper are not publicly available at this time but may be obtained from the authors upon reasonable request.

REFERENCES AND NOTES

1. U. M. Titulaer and R. J. Glauber, "Density operators for coherent fields," Phys. Rev. **145**, 1041–1050 (1966).
2. R. A. Campos, B. E. Saleh, and M. C. Teich, "Quantum-mechanical lossless beam splitter: Su(2) symmetry and photon statistics," Phys. Rev. A **40**, 1371–1384 (1989).
3. U. Leonhardt, "Quantum statistics of a lossless beam splitter: Su(2) symmetry in phase space," Phys. Rev. A **48**, 3265–3277 (1993).
4. M. Dakna, L. Knöll, and D.-G. Welsch, "Quantum state engineering using conditional measurement on a beam splitter," Eur. Phys. J. D **3**, 295–308 (1998).
5. H. Bauke and N. R. Itzhak, "Visualizing quantum mechanics in phase space," arXiv (2011).
6. O. Steuernagel, D. Kakofengitis, and G. Ritter, "Wigner flow reveals topological order in quantum phase space dynamics," Phys. Rev. Lett. **110**, 030401 (2013).
7. M. Oliva and O. Steuernagel, "Quantum Kerr oscillators' evolution in phase space: Wigner current, symmetries, shear suppression, and special states," Phys. Rev. A **99**, 032104 (2019).
8. W. F. Braasch, O. D. Friedman, A. J. Rimberg, *et al.*, "Wigner current for open quantum systems," Phys. Rev. A **100**, 012124 (2019).
9. Y.-R. Chen, H.-Y. Hsieh, J. Ning, *et al.*, "Experimental reconstruction of Wigner phase-space current," Phys. Rev. A **108**, 023729 (2023).

10. E. Wigner, "On the quantum correction for thermodynamic equilibrium," Phys. Rev. **40**, 749–759 (1932).
11. M. V. Berry and N. L. Balazs, "Evolution of semiclassical quantum states in phase space," J. Phys. A **12**, 625–642 (1979).
12. H. J. Korsch and M. V. Berry, "Evolution of Wigner's phase-space density under a nonintegrable quantum map," Physica D **3**, 627–636 (1981).
13. U. Leonhardt and H. Paul, "Measuring the quantum state of light," Prog. Quantum Electron. **19**, 89–130 (1995).
14. W. P. Schleich, *Quantum Optics in Phase Space* (Wiley, 2001).
15. W. H. Zurek, "Sub-Planck structure in phase space and its relevance for quantum decoherence," Nature **412**, 712–717 (2001).
16. T. L. Curtright, D. B. Fairlie, and C. K. Zachos, *A Concise Treatise on Quantum Mechanics in Phase Space* (World Scientific, 2014).
17. A. I. Lvovsky, "Squeezed light," arXiv [quant-ph] (2016).
18. D. Kakofengitis and O. Steuernagel, "Wigner's quantum phase space flow in weakly-anharmonic weakly-excited two-state systems," Eur. Phys. J. Plus **132**, 381 (2017).
19. M. Oliva and O. Steuernagel, "Dynamic shear suppression in quantum phase space," Phys. Rev. Lett. **122**, 020401 (2019).
20. J. Hancock, M. A. Walton, and B. Wynder, "Quantum mechanics another way," Eur. J. Phys. **25**, 525–534 (2004).
21. J. E. Moyal, "Quantum mechanics as a statistical theory," Proc. Cambridge Philos. Soc. **45**, 99–124 (1949).
22. H. J. Groenewold, "On the principles of elementary quantum mechanics," Physica **12**, 405–460 (1946).
23. M. Oliva, D. Kakofengitis, and O. Steuernagel, "Anharmonic quantum mechanical systems do not feature phase space trajectories," Physica A **502**, 201–210 (2018).
24. O. Steuernagel, P. Yang, and R.-K. Lee, "On the formation of lines in quantum phase space," J. Phys. A **56**, 015306 (2023).
25. M. S. Kim, W. Son, V. Bužek, *et al.*, "Entanglement by a beam splitter: nonclassicality as a prerequisite for entanglement," Phys. Rev. A **65**, 032323 (2002).
26. X.-B. Wang, "Theorem for the beam-splitter entangler," Phys. Rev. A **66**, 024303 (2002).
27. D. D. Nolte, "The tangled tale of phase space," Phys. Today **63**, 33–38 (2010).
28. There are several different formulations of quantum theory, Schrödinger's, Heisenberg's, the phase space formulations due to Wigner, Moyal, and Groenewold (and their offshoots due to Glauber and Sudarshan, Husimi, and others), Feynman's path integrals, the de Broglie–Bohm and many-worlds interpretation, spontaneous collapse models, and others. Here, we only use Wigner's formulation [42].
29. W. B. Case, "Wigner functions and Weyl transforms for pedestrians," Am. J. Phys. **76**, 937–946 (2008).
30. M. Hillery, R. F. O'Connell, M. O. Scully, *et al.*, "Distribution functions in physics: fundamentals," Phys. Rep. **106**, 121–167 (1984).
31. A. Donoso and C. C. Martens, "Quantum tunneling using entangled classical trajectories," Phys. Rev. Lett. **87**, 223202 (2001).
32. R. T. Skodje, H. W. Rohrs, and J. VanBuskirk, "Flux analysis, the correspondence principle, and the structure of quantum phase space," Phys. Rev. A **40**, 2894–2916 (1989).
33. Since only the divergence of the current enters the time evolution Eq. (1) [35], there can exist ambiguity since purely rotational vector fields can be added to the current $\boldsymbol{J}$, and other physical arguments might have to be employed in order to remove this ambiguity; for an example, see Ref. [7]. Here, this problem does not occur.
34. D. Cohen, "Lecture notes in quantum mechanics," arXiv (2018).
35. O. Steuernagel and R.-K. Lee, "Photon creation viewed from Wigner's phase space current perspective," arXiv (2023).
36. C. Kurtsiefer, T. Pfau, and J. Mlynek, "Measurement of the Wigner function of an ensemble of helium atoms," Nature **386**, 150–153 (1997).
37. P. Grangier, "Make it quantum and continuous," Science **332**, 313–314 (2011).
38. K. E. Cahill and R. J. Glauber, "Density operators and quasiprobability distributions," Phys. Rev. **177**, 1882–1902 (1969).
39. A. Royer, "Wigner function as the expectation value of a parity operator," Phys. Rev. A **15**, 449–450 (1977).
40. G. Manfredi and M. R. Feix, "Entropy and Wigner functions," Phys. Rev. E **62**, 4665–4674 (2000).
41. J. J. Włodarz, "Entropy and Wigner distribution functions revisited," Int. J. Theor. Phys. **42**, 1075–1084 (2003).
42. Out of all quantum phase space distributions [38] only Wigner's [30] yields the correct projections in Schrödinger's position $\varrho(x,x,t)=\int \mathrm{d}p\, W(x,p,t)$ and momentum densities $\tilde{\varrho}(p,p,t)=\int \mathrm{d}x\, W(x,p,t)$, while giving the overlap between states in the simple form $|\langle\psi_1(x,t)|\psi_2(x,t)\rangle|^2=2\pi\hbar\int\int \mathrm{d}x\mathrm{d}p W_1(x,p,t)W_2(x,p,t)$. We therefore consider Wigner's approach [10] as special and intuitive, so we use it exclusively.
43. U. Leonhardt, "Quantum physics of simple optical instruments," Rep. Prog. Phys. **66**, 1207–1249 (2003).
44. M. Veronez and M. A. M. de Aguiar, "Phase space flow in the Husimi representation," J. Phys. A **46**, 485304 (2013).
45. I. F. Valtierra, A. B. Klimov, G. Leuchs, *et al.*, "Quasiprobability currents on the sphere," Phys. Rev. A **101**, 033803 (2020).
46. W. Heisenberg, "Über den anschaulichen inhalt der quantentheoretischen kinematik und mechanik," Z. Phys. **43**, 172–198 (1927).
47. R. Cabrera, D. I. Bondar, K. Jacobs, *et al.*, "Efficient method to generate time evolution of the Wigner function for open quantum systems," Phys. Rev. A **92**, 042122 (2015).
48. M. Ćirić, D. I. Bondar, and O. Steuernagel, "Exponential unitary integrators for nonseparable quantum Hamiltonians," Eur. Phys. J. Plus **138**, 1 (2023).
49. C. K. Hong, Z. Y. Ou, and L. Mandel, "Measurement of subpicosecond time intervals between two photons by interference," Phys. Rev. Lett. **59**, 2044–2046 (1987).
50. T. Takabayasi, "The formulation of quantum mechanics in terms of ensemble in phase space," Prog. Theo. Phys. **11**, 341–373 (1954).